Physiol Genomics 39: 195–201, 2009.
First published August 11, 2009; doi:10.1152/physiolgenomics.00100.2009.

Clinical and molecular characterizations of novel *POU3F4* mutations reveal that DFN3 is due to null function of POU3F4 protein

Hee Keun Lee,[1]* Mee Hyun Song,[2,7]* Myengmo Kang,[3] Jung Tae Lee,[4] Kyoung-Ah Kong,[3] Su-Jin Choi,[1] Kyu Yup Lee,[5] Hanka Venselaar,[6] Gert Vriend,[6] Won-Sang Lee,[7] Hong-Joon Park,[8] Taeg Kyu Kwon,[4] Jinwoong Bok,[3] and Un-Kyung Kim[1]

[1]*Department of Biology, Kyungpook National University, Daegu;* [2]*Department of Otorhinolaryngology, Kwandong University College of Medicine, Goyang;* [3]*Department of Anatomy, Brain Korea 21 Project for Medical Science, Yonsei University College of Medicine, Seoul;* [4]*Department of Immunology, Keimyung University School of Medicine;* [5]*Department of Otorhinolaryngology-Head and Neck Surgery, College of Medicine, Kyungpook National University, Daegu, South Korea;* [6]*Radboud University Nijmegen Medical Centre, Nijmegen, The Netherlands;* [7]*Department of Otorhinolaryngology, Yonsei University College of Medicine; and* [8]*Soree Ear Clinic, Seoul, South Korea*

Submitted 15 June 2009; accepted in final form 4 August 2009

Lee HK, Song MH, Kang M, Lee JT, Kong K, Choi SJ, Lee KY, Venselaar H, Vriend G, Lee WH, Park HJ, Kwon TK, Bok J, Kim UK. Clinical and molecular characterizations of novel *POU3F4* mutations reveal that DFN3 is due to null function of POU3F4 protein. *Physiol Genomics* 39: 195–201, 2009. First published August 11, 2009; doi:10.1152/physiolgenomics.00100.2009.—X-linked deafness type 3 (DFN3), the most prevalent X-linked form of hereditary deafness, is caused by mutations in the *POU3F4* locus, which encodes a member of the POU family of transcription factors. Despite numerous reports on clinical evaluations and genetic analyses describing novel *POU3F4* mutations, little is known about how such mutations affect normal functions of the POU3F4 protein and cause inner ear malformations and deafness. Here we describe three novel mutations of the *POU3F4* gene and their clinical characterizations in three Korean families carrying deafness segregating at the DFN3 locus. The three mutations cause a substitution (p.Arg329Pro) or a deletion (p.Ser310del) of highly conserved amino acid residues in the POU homeodomain or a truncation that eliminates both DNA-binding domains (p.Ala116fs). In an attempt to better understand the molecular mechanisms underlying their inner ear defects, we examined the behavior of the normal and mutant forms of the POU3F4 protein in C3H/10T1/2 mesodermal cells. Protein modeling as well as in vitro assays demonstrated that these mutations are detrimental to the tertiary structure of the POU3F4 protein and severely affect its ability to bind DNA. All three mutated POU3F4 proteins failed to transactivate expression of a reporter gene. In addition, all three failed to inhibit the transcriptional activity of wild-type proteins when both wild-type and mutant proteins were coexpressed. Since most of the mutations reported for DFN3 thus far are associated with regions that encode the DNA binding domains of POU3F4, our results strongly suggest that the deafness in DFN3 patients is largely due to the null function of POU3F4.

hearing loss; X-linked deafness type 3; inner ear

CONGENITAL HEARING LOSS IS one of the most common sensory disorders in humans, affecting approximately one in 1,000 newborns (24). More than 50% of the congenital hearing loss is due to genetic causes, and the majority of these hereditary cases are nonsyndromic. While most genetic nonsyndromic hearing loss is caused by mutations in autosomal genes, X-linked cases are estimated to comprise between 1 and 5% of these (26). Thus far, four different X-linked nonsyndromic hearing loss loci (DFN2, DFN3, DFN4, and DFN6) have been mapped, but the causative gene has been identified only for the DFN3 locus (33).

X-linked deafness type 3 (DFN3) accounts for ~50% of all families carrying X-linked nonsyndromic hearing loss (26). Clinical characteristics of DFN3 in affected males include temporal bone abnormalities, stapes fixation, and, in most cases, a mixed type of hearing loss, which is often progressive (7, 8, 10). Anatomical anomalies of the temporal bone revealed by computer-assisted tomography (CT) include dilatation of the lateral end of the internal acoustic canal (IAC), abnormally wide communication between the IAC and inner ear compartment, and, sometimes, partial hypoplasia of the cochlea (8, 27). As a result of the widening of the bony IAC, cerebrospinal fluid can enter the vestibule, which is thought to underlie the reported "gusher" phenomenon, described as fluid gushing out upon removal of the stapes footplate during corrective surgery (8). Female carriers of a mutation in the DFN3 locus typically show little or no hearing loss (26).

Deafness segregating at the DFN3 locus is associated with mutations in the *POU3F4* gene (11). POU3F4 belongs to a superfamily of POU domain transcription factors, which are characterized by a conserved bipartite DNA binding domain. This domain consists of a POU-specific domain and a POU homeodomain, both of which are helix-turn-helix structural motifs that influence DNA binding and specificity (22). Studies using *POU3F4* murine ortholog (*Brn-4/Pou3f4*) showed that the Pou3f4 protein binds to DNA on the POU-specific binding motif and regulates downstream target genes (22). Expression of *Pou3f4* is found broadly in the developing neural tube during embryogenesis but is restricted to the forebrain in adults (20, 22). *Pou3f4* has also been shown to be expressed in the limb muscle, pancreas, and inner ear (12, 17, 28, 29). During inner ear development, *Pou3f4* expression is exclusively detected in the mesenchymal tissue adjacent to the otic epithelium (28, 29). Targeted deletion of *Pou3f4* in mice results in abnormalities mainly in the mesenchyme-derived structures such as the spiral limbus, the scala tympani, and strial fibrocytes of the cochlea, as well as defects in the temporal bone (23, 29). In addition, *Pou3f4* knockout mice also display malformations in tissues that do not normally express *Pou3f4* such as the stapes of the middle ear and the membranous components of the cochlea, indicating possible roles of Pou3f4

* H. K. Lee and M. H. Song contributed equally to this work.

Addresses for reprint requests and other correspondence: J. Bok, Dept. of Anatomy, Brain Korea 21 Project for Medical Science, Yonsei Univ. College of Medicine, Seoul, South Korea (e-mail: bokj@yuhs.ac) or U.-K. Kim, Dept. of Biology, Kyungpook Natl. Univ., Daegu, South Korea (e-mail: kimuk@knu.ac.kr).

in reciprocal interactions between peri-otic mesenchyme and other tissues such as the otic epithelium (29).

Numerous genetic analyses of DFN3 families have identified mutations in the *POU3F4* gene. These include intragenic mutations, partial or complete deletions of the gene, as well as deletions, inversions, and duplications of the *POU3F4* genomic region not encompassing the *POU3F4* coding sequence (8). Clinical characterizations of affected individuals and their specific mutations in *POU3F4* have also been described (8). Nevertheless, little is known about how such mutations affect the normal function of the POU3F4 protein, which leads to the characteristic inner ear defects and deafness. Nor is it known how POU3F4 contributes to the normal development of the inner ear.

Here we report three novel mutations in the *POU3F4* gene identified in three Korean families carrying X-linked hereditary hearing loss and the clinical characterization of affected family members. In addition, we performed molecular modeling and various in vitro assays to understand the molecular basis of the inner ear defects caused by these mutations.

MATERIALS AND METHODS

Subjects and clinical evaluations. Two Korean families exhibiting an X-linked inheritance pattern and one Korean family in which X-linked inheritance was plausible were ascertained at the Department of Otorhinolaryngology, Yonsei University College of Medicine, Seoul, South Korea. The proband of each family was subjected to detailed clinical evaluations including medical history, otologic examinations, audiologic testing, and CT of the temporal bone. The clinical evaluations were also performed on other members of the families, including affected males and the female carriers. For audiologic testing, either brainstem-evoked response audiometry (BERA) or pure tone audiometry (PTA) was performed in line with the age of the patient, and the pure tone average was calculated with the thresholds at 0.5, 1, 2, and 4 kHz. High-resolution temporal bone CT was performed with a 16 row multi-detector CT scanner (SOMATOM Sensation 16; Siemens, Erlangen, Germany) by using a standard temporal bone protocol (18). Contiguous 0.7-mm scans of the temporal bone were acquired in the axial plane and reformatted coronally with 1.0-mm increments. Written informed consent was obtained from participating individuals, and this study was approved by the Institutional Review Board of the Yonsei University College of Medicine.

Genetic analyses. For linkage analyses, genomic DNAs from the families were extracted from peripheral blood using the FlexiGene DNA extraction kit (Qiagen). They were genotyped with centromeric microsatellite marker DXS986 (57.36 cM from Marshfield Map) and telomeric maker DXS6803 (57.91 cM from Marshfield Map) flanking the DFN3 locus (Xq21.1) using standard PCR conditions. The coding region of *POU3F4* was amplified for direct sequencing using three sets of primers: *1*) forward primer 5′-GTAACCCGTGCTAGCGTCTT-3′ and reverse primer 5′-GTCGGAGTGATCCTGGCAAT-3′, *2*) forward primer 5′-CACTCACCGCACACTAACCA-3′ and reverse primer 5′-ACACGCACCACTTCCTTCTC-3′, *3*) forward primer 5′-CTCCATCGAGGTGAGTGTCA-3′ and reverse primer 5′-GGAGCCAGGAATATGAGATCC-3′. The amplified DNA fragments were sequenced with an ABI PRISM Big Dye Terminator Cycle Sequencing Kit (V3.1) and an ABI PRISM 3130XL DNA analyzer (Applied Biosystems). Data were analyzed by using ABI Sequencing Analysis (v.5.0) and Lasergene-SeqMan software. The resulting sequences were compared with the *POU3F4* sequence from GenBank (accession no. NM_000307). We also sequenced 70 Koreans with normal hearing to determine whether the mutations were presented in the unaffected Korean population.

Molecular modeling. The crystal structure of POU2F1/Oct-1 was used as a template to build a model of wild-type and mutant POU3F4 proteins. Modeling was performed with the WHAT IF software (34) with standard parameter settings and protocols as described previously (4, 9). The details of the modeling protocol, including files used, sequence alignment, parameter choices, etc., are available from http://www.cmbi.ru.nl/~hvensela/pou3f4/.

Plasmid construction. To construct expression vectors for wild-type and mutant POU3F4 proteins, the full-length open reading frame (ORF) of the single-exon *POU3F4* gene was amplified by PCR from the genomic DNA of normal or affected males and sub-cloned into the pcDNA3 expression vector. The primer pairs used were 5′-atgaattcatggccacagctgcctcg-3′ and 5′-atcggccgctcagagatcatggcaag-3′. Oligonucleotides encoding the hemagglutinin (HA) epitope were also inserted at the 5′ of the *POU3F4* ORF.

Immunocytochemistry. C3H10T1/2 cells grown on a LabTek 8 chamber slide were transfected with either wild-type or mutant POU3F4 expression plasmids, together with EGFP plasmid. Forty-eight hours later, the cells were fixed with 4% paraformaldehyde for 10 min and permeabilized by 0.5% Triton for 10 min at room temperature. The cells were then incubated sequentially with monoclonal anti-HA antibody (Zymed) overnight at 4°C, AlexaFluor 568 anti-mouse IgG antibody (Invitrogen) for 1 h at room temperature, and 4′, 6′-diamidino-2-phenylindole for 5 min at room temperature. Images of the immunostained cells were taken with Olympus IX70 fluorescent microscope equipped with Olympus DP70 camera (Zeiss) and processed using Adobe Photoshop (Adobe Systems). To determine the percentages of the cells expressing POU3F4 proteins outside the nucleus, 100–200 cells from each chamber were counted manually by an investigator blind to the sample identities. Graphs were plotted based on the numbers collected from at least three independent experiments.

Expression and purification of recombinant POU3F4 protein. A glutathione S-transferase (GST) recombinant POU3F4 plasmid was constructed by subcloning the digested fragment containing whole POU3F4 sequences into pGEX-4T-1 *Kpn*I/*Eco*RI site. GST fusion proteins were purified from the respective *Escherichia coli* BL21 extracts with glutathione-Sepharose (Pharmacia, Piscataway, NJ) according to standard procedures (14).

Electrophoretic mobility shift assay. The sequences of the double-stranded oligonucleotides used to detect the DNA-binding activities of POU3F4 were as follows: 5′-CAATATGCTAATCAATATGCTAAT-3′. The reaction mixture for electrophoretic mobility shift assay (EMSA) contained 20 mM Tris·HCl, pH 7.6, 1 mM dithiothreitol, 2 mM $MgCl_2$, 1 mM EDTA, 10% glycerol, 1% NP-40, 1 μg poly(dI-dC), and 2 μg purified recombinant GST-POU3F4 fusion proteins. Unlabeled oligonucleotides were added into the reaction mixture and incubated for 10 min at room temperature. [^{32}P]-labeled probe DNA (300,000 cpm) was added, and the binding reaction was allowed to proceed for another 20 min. Mixtures were resolved on 8% polyacrylamide gels at 150 V for 4 h. Gels were dried and subjected to autoradiography.

Transcription reporter assays. The luciferase reporter plasmids were constructed by inserting either the upstream promoter region of human *POU3F4* gene (−482 to +25), or two or three copies of the Pou3f4 binding element (CAATATGCTAAT) into the pGL2 basic vector (21). C3H10T1/2 cells plated in 24-well plates were cotransfected with 300 ng of either wild-type or mutant POU3F4 expression plasmid, or both plasmids together, 150 ng of the luciferase reporter plasmid, and 20 ng of SV40-renilla plasmid for the transfection efficiency control. The transfected cells were incubated for 24 h and subjected to the luciferase assay according to the manufacturer's protocol (Promega). Transfection efficiencies in each condition were normalized with renilla luciferase activity, which was under the control of a SV-40 promoter. Results were plotted based on at least three independent experiments.

RESULTS

Clinical characterizations of families carrying X-linked deafness. The pedigree of family SV08-18 showed a typical X-linked recessive inheritance pattern of hearing loss (Fig. 1*A*).

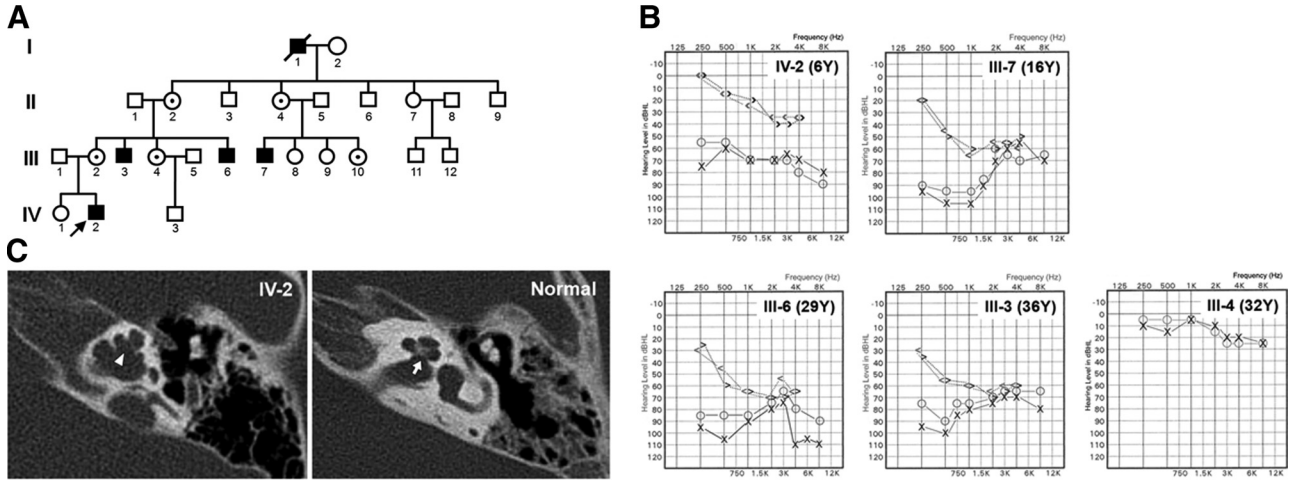

Fig. 1. Clinical characterizations of the family SV08-18 showing X-linked hereditary hearing loss. *A*: pedigree showing a typical X-linked recessive inheritance pattern of hearing loss. Square (male), circle (female), shaded (affected individual), slashed (deceased), circle with a dot (female mutation carrier), arrow (the proband of the family). *B*: audiograms of the proband (IV-2, 6 yr) with a severe mixed hearing loss and older male members with worse hearing are shown. A female carrier (III-4, 32 yr) shows normal hearing. ○ (*right*) × (*left*): air conduction threshold. < (*right*) > (*left*): bone conduction threshold. dBHL, decibel hearing level. *C*: high resolution computer-assisted tomographic (CT) scans of the temporal bones of the proband (IV-2) shows characteristic findings of X-linked deafness type 3 (DFN3) such as fistulous connection between the basal turn of cochlea and internal auditory canal and defective cochlear modiolus (*left* panel, arrowhead), unlike the normal appearance of cochlear modiolus in the normal temporal bone (*right* panel, arrow).

PTA measurements indicated that the proband of this family (IV-2, 6 yr) had a severe mixed type of hearing loss (Fig. 1*B*). Three other affected older males (III-3, 36 yr; III-6, 29 yr; III-7, 16 yr) also showed similar patterns of hearing loss, but the thresholds were higher than that of the proband (Fig. 1*B*). Although longitudinal data on hearing loss were not available for these male family members, more severe hearing loss shown in older males especially in the sensorineural component suggested progressiveness of hearing impairment, as previously reported (8). Two female carriers in the family (III-2, III-4) had normal hearing (Fig. 1*B*).

The second family, SV08-17, also showed a typical X-linked recessive inheritance pattern of hearing loss: five males being affected in three generations (Suppl. Fig. S1).[1] The proband was diagnosed with severe hearing loss by BERA [thresholds >60 dB nHL (decibel normal hearing level)] 1 mo after birth and is in the process of auditory rehabilitation with hearing aids. Another affected male in the family (II-4, 23 yr) was also diagnosed with hearing loss at the age of 6 yr and developed only limited verbal communication with hearing aids.

In the third family, SV08-21, the proband was diagnosed with severe hearing loss by BERA (75 and 90 dB nHL on the right and left side, respectively) at the age of 2 yr (Suppl. Fig. S1). Audiologic testing was not available for other members of the family, although the granduncle of the proband had suspected hearing loss. Since the proband and his mother carried the same mutation, the hearing loss appeared to be inherited in an X-linked recessive pattern in this family (Fig. 2; data not shown).

Further CT scans performed on six patients from all three families revealed that the defects of the temporal bones were comparable for all the patients examined and were characteristic of DFN3 (8, 27), including a wide fistulous connection between the basal turn of the cochlea and the IAC, and defects in the cochlear modiolus (Fig. 1*C*; data not shown). No other medical or neurological deficits were identified in any of the affected family members.

Linkage and mutation analyses. Since the family histories and clinical evaluations of all three families were characteristic for DFN3, we performed linkage analyses using DXS986 and DXS6803 microsatellite markers. Deafness showed linkage to the DFN3 locus in these families (Suppl. Fig. S1), so we searched for mutations in the *POU3F4* gene in the affected members of the families by directly sequencing the *POU3F4* coding region. Sequence analyses in family SV08-18 revealed a point mutation at nucleotide 986, guanine to cytosine (c.986 G>C) (Fig. 2*A*). This nucleotide change converts an arginine to a proline at the amino acid position 329 (p.R329P), which is one of the most conserved residues in the POU homeodomain of the POU3F4 protein (Fig. 2*E*).

Sequence analyses of family SV08-17 identified a one-base pair (bp) deletion at nucleotide position 346 (c.346delG) (Fig. 2*B*). This mutation causes a frame shift that encodes 25 new amino acids followed by premature termination of the protein at amino acid position 141 (p.Ala116fs). This results in a truncated form of the POU3F4 protein lacking both DNA binding domains (Fig. 2*D*).

The affected members of family SV08-21 had an in-frame deletion of three nucleotides (c.927-929delCTC; Fig. 2*C*), resulting in a deletion of the amino acid serine (p.S310del) in the POU homeodomain (Fig. 2*C*).

Structural analyses of the wild-type and mutant POU3F4 proteins. The POU3F4 protein consists of an NH_2-terminal domain important for transcriptional activity and two COOH-terminal DNA-binding domains. These DNA-binding domains consist of the POU-specific domain connected by a short linker region to the POU homeodomain (13, 20, 22) (Fig. 2*D*). All three mutations identified in this study were expected to affect DNA binding activity of the POU3F4 protein, because they affect one of these domains. To examine the effect of the mutations on

[1] The online version of this article contains supplemental material.

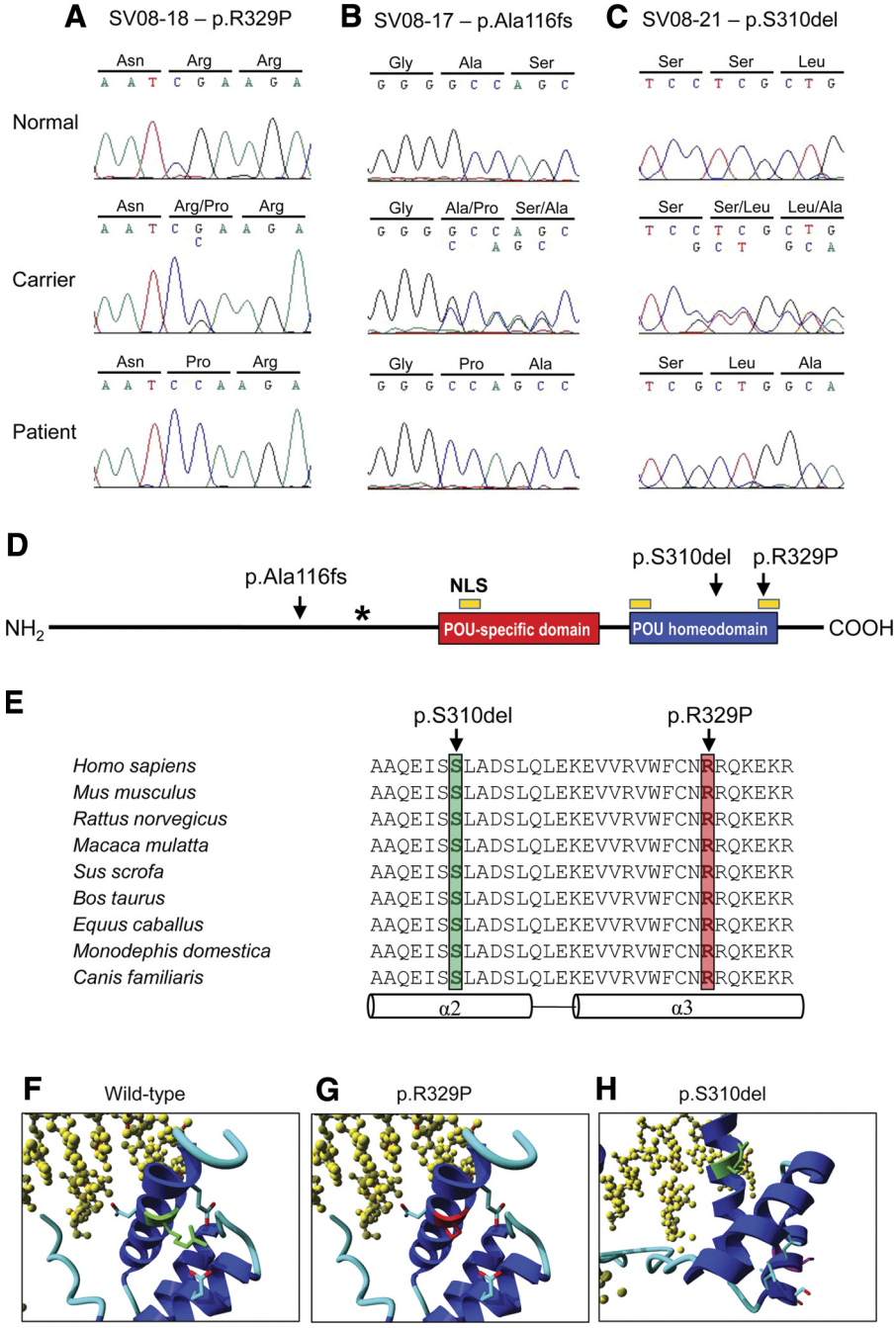

Fig. 2. Three novel mutations in *POU3F4* locus are expected to affect protein-DNA interaction of POU3F4 protein. *A–C*: novel mutations identified in 3 Korean families carrying X-linked hereditary deafness. *A*: family SV08-18 carries a mutation of G to C at nucleotide position 986, which results in a conversion of arginine to proline at the amino acid position 329 (p.R329P). This G-to-C change is observed in all affected males, and G/C heterozygosity was detected in all female carriers. *B*: a 1 bp deletion identified in family SV08-17 causes a frame shift of 26 amino acids starting from alanine at the amino acid position 116, followed by a truncation (p.Ala116fs). *C*: a deletion of 3 nucleotides from position 927 to 929 detected in family SV08-21 causes a single amino acid deletion (p.S310del) without affecting the coding frame. *D*: schematic illustration of POU3F4 protein labeled with the 3 novel mutations identified in this study. POU-specific and homeodomain are shown as red and blue boxes, respectively, and 3 putative nuclear localization signals (NLS) are indicated as yellow boxes above the POU-specific or POU homeodomain. The positions of the mutation are indicated with arrows, and the location of premature termination in p.Ala116fs mutation is marked by an asterisk. p.R329P mutation is located in one of the putative NLSs in the POU homeodomain. *E*: alignment of the amino acid sequence of the 2nd and 3rd α-helices in the POU3F4 proteins from several eukaryotes. Amino acid sequence in this region is highly conserved in mammals. *F–H*: molecular modeling of the wild-type and mutant POU3F4 proteins. *F*: the 3rd helix in the POU homeodomain is illustrated. The green amino acid residue is Arg329. DNA is shown in a yellow ball-and-stick representation. *G*: p.R329P mutation located in the 3rd α-helix of the POU homeodomain is expected to destabilize the helical structure, affecting the proper protein-DNA interactions. The 2 glutamates that had an interaction with the lost arginine are shown, as is the asparagine that makes important, specificity-relating DNA contacts. *H*: in the p.S310del mutant, the lack of one amino acid residue will cause a shift of one position for all subsequent residues, disrupting normal interactions. The details of the modeling are also available from http://www.cmbi.ru.nl/~hvensela/pou3f4/.

the tertiary structure of the POU3F4 protein, molecular models of wild-type, p.R329P, and p.S310del POU3F4 proteins were built based on the known crystal structure of the POU2F1/Oct-1 protein (19).

The p.R329P mutation is located in the third α-helix of the POU homeodomain, which is crucial for protein-DNA interactions (Fig. 2, *E–G*). The substitution of proline for the normal arginine at this position is expected to be detrimental to the α-helix structure due to destabilization of two important salt-bridges as well as loss of a series of hydrophobic contacts. In addition, the amino acid side chain structure of proline typically inserts an obligate bend that disrupts α-helical structures. Such disturbances generally tend to massively reduce the proper protein-DNA interactions.

The serine residue at position 310 is located in the middle of the second α-helix of the POU homeodomain (Fig. 2*E*). This helix is not in direct contact with the DNA but is likely important for the overall structure of the POU homeodomain. The homology model suggests that α-helical structure will remain after deletion of the serine residue (p.S310del) (Fig. 2*H*). However, since the absence of one residue will cause a shift of one position for the subsequent residues in this helix, this will have dramatic effects on the stability of this helix because several hydrophobic interactions will get lost and a polar residue will become buried in the hydrophobic core of the protein. As a result, the interaction with the other helices is disturbed and the overall stability of the domain is decreased, which will severely reduce its DNA binding ability.

Effects of the POU3F4 mutations on DNA binding activity. Our modeling study suggested that all three mutations identified in DFN3 patients are likely affecting DNA binding ability by altering the tertiary structure of the DNA binding domains of the POU3F4 protein. To test this possibility, we conducted EMSA. Expression vectors encoding wild-type and mutant forms of POU3F4 protein were constructed, and the proteins were translated in vitro. The DNA-binding abilities of the in vitro translated and purified POU3F4 proteins were tested with the oligonucleotide probe (CAATATGCTAAT) that has been shown to specifically bind the murine Pou3f4 proteins (21). As shown in Fig. 3*A*, wild-type POU3F4 proteins bound strongly to the labeled oligonucleotides to form protein-DNA complexes (Fig. 3*A*, arrow). Specificity of the protein-DNA interaction was confirmed by competition experiments, in which addition of unlabeled oligonucleotide probes completely abolished the protein-DNA interactions. In contrast to the wild-type POU3F4, no detectable protein-DNA complexes were observed with any of the mutant forms of POU3F4. These results indicate that the mutations severely compromise the ability of the POU3F4 proteins to bind target DNA sequences.

Effects of the POU3F4 mutations on subcellular localization. The computer program "predictNLS" (5) predicts three putative nuclear localization signal (NLS) motifs in wild-type POU3F4. One of these is located in the POU-specific domain and the other two are in the POU homeodomain (Fig. 2*D*). The p.R329P mutation is located in one of the NLS motifs in the POU homeodomain, and the p.S310del mutation is located between the two NLSs in the POU homeodomain (Fig. 2*D*). The truncating mutation (p.Ala116fs) results in a protein that does not have any of the NLS motifs due to the lack of the DNA binding domains.

To determine how these mutations affect nuclear localization of the POU3F4 proteins, expression vectors encoding wild-type or mutant POU3F4 proteins fused with the HA epitope were transiently expressed in the C3H10T1/2 cells (30). We chose this mouse mesenchymal cell line since *Pou3f4* is mainly expressed in the mesenchyme surrounding the developing inner ear (28). Immunofluorescent analyses using anti-HA or anti-POU3F4 antibodies showed that wild-type POU3F4 proteins were localized exclusively in the nuclei of transfected cells (Fig. 3*B*; data not shown). In contrast, the majority of p.R329P or p.Ala116fs POU3F4 proteins, in which at least one NLS motif is disrupted, were found in both the cytoplasm and the nucleus (Fig. 3*B*). Although we expected normal nuclear localization for the p.S310del mutant, which preserved all three putative NLS motifs, POU3F4 proteins with this mutation also lost their normal subcellular localization and were found throughout the cells. This mislocalization could be due to the changes in the tertiary structure of the POU homeodomain where the NLS domains reside.

Effects of the POU3F4 mutations on transcriptional activities. The inability of the mutant POU3F4 proteins to bind to the target DNA sequence or to correctly localize in the nucleus strongly suggested that the transcriptional activity of the mutant POU3F4 proteins would also be severely compromised. To test this, we constructed a reporter plasmid, in which expression of the firefly luciferase gene is regulated by the promoter region (from −472 to +25 bp) of the human *POU3F4* gene, which has been shown to be directly regulated by the POU3F4 protein itself (21). The reporter plasmid was cotransfected with the plasmid encoding either wild-type or mutant POU3F4 into C3H10T1/2 cells, and the ability of each POU3F4 protein to transactivate the reporter gene was assessed

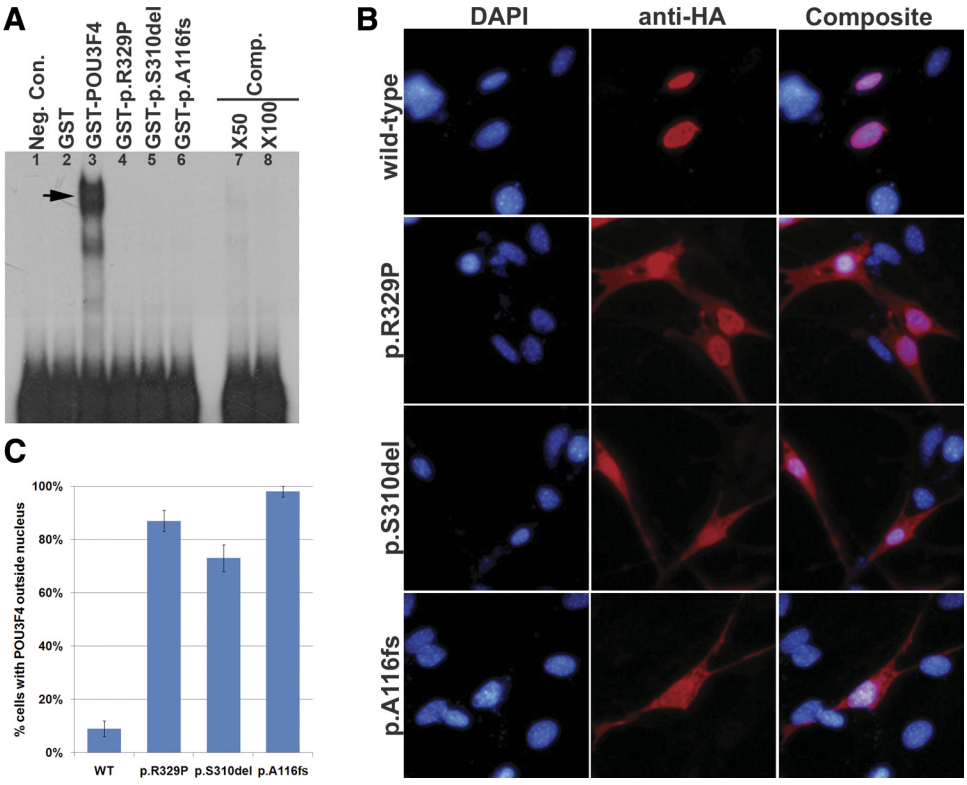

Fig. 3. DNA-binding ability and subcellular localization were disrupted by the POU3F4 mutations. *A*: electrophoretic mobility shift assay (EMSA). Wild-type POU3F4 proteins formed a protein-DNA complex with the labeled oligonucleotides (*lane 3*, arrow), which were completely disrupted by adding unlabeled oligonucleotides as competitors (*lanes 7, 8*). In contrast, p.R329P (*lane 4*), p.S310del (*lane 5*), or p.A116fs (*lane 6*) mutant proteins failed to bind to the DNA molecules. *B*: immunocytochemical analyses with anti-hemagglutinin (HA) antibody of wild-type and mutant POU3F4 proteins transiently expressed in C3H10T1/2 cells. While wild-type POU3F4 proteins were mostly localized inside the nucleus, most of the mutant POU3F4 proteins were found in both the nucleus and cytoplasm. *C*: graph quantifying the percentage of cells expressing the POU3F4 proteins outside the nucleus.

by measuring the luciferase activity in the transfected cells. In this system, wild-type POU3F4 protein activated the reporter gene expression almost threefold, but all three mutant POU3F4 proteins failed to activate the gene expression (Fig. 4*B*), indicating that the *POU3F4* mutations completely abolish the transcriptional activity of POU3F4 proteins. Similar effects were observed with another reporter construct whose luciferase expression is under the control of two or three copies of the POU3F4 recognition element (CAATATGCTAAT) (21) (data not shown). Next, we tested to see if the mutant POU3F4 proteins could act as dominant-interfering variants. When both wild-type and any of the mutant POU3F4 proteins were coexpressed, the reporter expression activated by wild-type POU3F4 protein was not affected, indicating that the mutant POU3F4 proteins did not inhibit normal transcriptional activity of wild-type proteins (Fig. 4*B*). These results demonstrate that the three mutations identified in the DFN3 patients cause functional nulls of the POU3F4 protein.

DISCUSSION

We identified three novel mutations in the *POU3F4* gene in three Korean families displaying X-linked inheritance of hearing loss. Two of the mutations (p.R329P and p.S310del) occur in the POU homeodomain, and the third mutation (p.Ala116fs) causes a premature termination, resulting in a protein lacking the entire DNA-binding domains (Fig. 2). Like the three mutations we have studied here, most of the *POU3F4* mutations identified in DFN3 patients specify amino acid changes in regions that encode the DNA-binding domains, the majority being in the POU homeodomain (8), suggesting that loss of DNA binding ability may be a common pathological mechanism at the molecular level. Indeed, protein modeling and several molecular analyses demonstrate that the *POU3F4* mutations severely disrupt the DNA-binding ability of POU3F4, thereby completely abolishing the transcriptional activity of the protein (Figs. 3 and 4). The mutant POU3F4 proteins failed to inhibit normal transcriptional activity of wild-type POU3F4, excluding the possibility that the mutant proteins act as dominant-interfering variants. Overexpression of the mutant POU3F4 proteins in C3H10T1/2 cells did not seem to have any obvious deleterious effects on normal cell behaviors such as cell proliferation or cell death (data not shown). Together, these observations strongly suggest that the hearing loss in DFN3 is caused by the loss of function of POU3F4 protein, rather than by gain of ectopic functions of mutant proteins. Clinical evaluations of DFN3 patients in this study are consistent with previously published reports that demonstrated no clear genotype-phenotype correlation between the different types of the *POU3F4* mutations and the inner ear (26).

Mutations in *POU4F3*, another POU domain transcription factor, have been implicated in autosomal dominant hearing loss DFNA15 (32). Similar to our POU3F4 results, molecular analyses of *POU4F3* mutations identified in DFNA15 patients showed that the mutant POU4F3 proteins lack transcriptional activity due to the loss of nuclear localization and DNA-binding ability (6, 35). Thus, the two POU family transcription factors share a common molecular pathological mechanism, whereby transcription of target genes essential for inner ear development is affected. Consistent with its expression in the hair cells, POU4F3 has been shown to regulate genes important for hair cell differentiation such as *Gfi1* and *Lhx3* (15, 16). Similarly, the hearing loss in DFN3 by *POU3F4* mutations is most likely associated with lack of expression of downstream target gene(s) that plays critical roles in inner ear development, especially in the mesenchymal remodeling and otic epithelial-mesenchymal interactions. Only a few target genes of POU3F4 have been identified to date in other tissues: proglucagon gene in the α-cells of the pancreas (17), D1A dopamine receptor gene in the striatum (25), and human involucrin gene in the epidermis (36). However, little is known about downstream targets of POU3F4 in the peri-otic mesenchyme where *Pou3f4* is actively expressed (28). The temporal bone CT scans of DFN3 patients as well as the *Pou3f4* knockout inner ear phenotypes suggest that most of the inner ear malformations were found in the structures derived from the mesenchyme (23, 28). Therefore, elucidating the downstream targets of POU3F4 in the peri-otic mesenchyme will be crucial to understand how POU3F4 normally contributes to the mesenchymal patterning in inner ear development.

While the genes regulated by POU3F4 are unclear, previous studies provided hints as to how the *POU3F4* gene is regulated in the peri-otic mesenchyme during inner ear development. *TBX1*, a member of the T-box gene family of transcription factors and known causative gene for DiGeorge syndrome, is expressed in both the otic epithelium and peri-otic mesenchyme (1). Studies using tissue-specific knockout mice suggest that *Tbx1* expressed in the mesenchyme is required for the mesenchymal expression of *Pou3f4* (1), although it is not clear if Tbx1 directly regulates the mesenchymal *Pou3f4* expression. Consistent with this, a genetic interaction between *Tbx1* and *Pou3f4* has been demonstrated to be necessary for normal cochlear formation (3). Interestingly, expressions of both *Tbx1* and *Pou3f4* in the mesenchyme are dependent on Sonic hedgehog (31). Thus, a molecular pathway of *Shh-Tbx1-Pou3f4* in

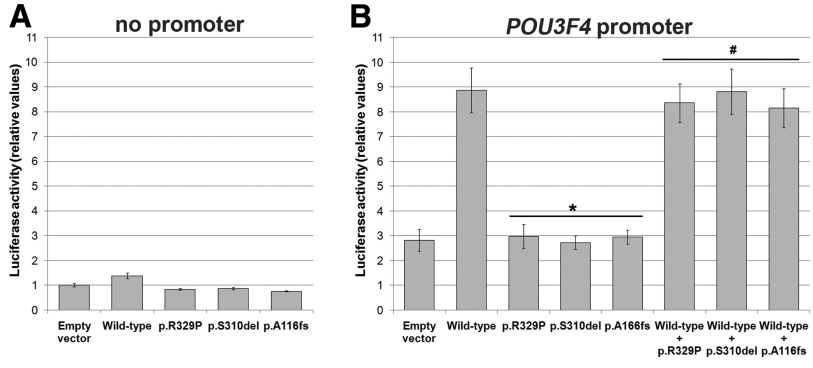

Fig. 4. Transcriptional activity of POU3F4 was abolished by the *POU3F4* mutations. *A*: luciferase activities in cells cotransfected with various POU3F4 proteins and the promoter-absent reporter construct. No luciferase activity was observed in cells expressing either wild-type or mutant POU3F4 proteins. *B*: luciferase activities in cells cotransfected with the reporter construct containing the POU3F4 promoter region (from −472 to +25 bp) and various forms of POU3F4 proteins. Wild-type POU3F4 protein upregulated the reporter gene expression, while none of the mutant POU3F4 proteins did. Cotransfection of the wild-type and any of the mutants induced luciferase activities comparable to the level activated by the wild type alone. *Significantly different from wild type (t-test, $P < 0.001$); #not significantly different from wild type ($P > 0.1$).

the peri-otic mesenchyme has been proposed to be involved in the normal cochlear patterning (2). Further analyses of the molecular networks regulating *POU3F4* as well as downstream genes regulated by *POU3F4* are warranted to produce a better understanding of the roles of POU3F4 in normal inner ear patterning, as well as the causative mechanism of DFN3.

ACKNOWLEDGMENTS

We thank Drs. Dennis T. Drayna and Doris K. Wu for critical reading of the manuscript. We also thank Jin Ahn for technical assistance.

GRANTS

This work is supported by Korea Healthcare Technology R&D Project, Ministry for Health, Welfare and Family Affairs, Republic of Korea, Grant A080588 (J. Bok, U.-K. Kim), by a research grant of the Life Insurance Philanthropy Foundation, by the Korean Ministry of Education through the Brain Korea 21 project (H. K. Lee, S.-J. Choi), and by The Netherlands Bioinformatics Centre (H. Venselaar).

REFERENCES

1. **Arnold JS, Braunstein EM, Ohyama T, Groves AK, Adams JC, Brown MC, Morrow BE.** Tissue-specific roles of Tbx1 in the development of the outer, middle and inner ear, defective in 22q11DS patients. *Hum Mol Genet* 15: 1629–1639, 2006.
2. **Bok J, Chang W, Wu DK.** Patterning and morphogenesis of the vertebrate inner ear. *Int J Dev Biol* 51: 521–533, 2007.
3. **Braunstein EM, Crenshaw EB 3rd, Morrow BE, Adams JC.** Cooperative function of Tbx1 and Brn4 in the periotic mesenchyme is necessary for cochlea formation. *J Assoc Res Otolaryngol* 9: 33–43, 2008.
4. **Chinea G, Padron G, Hooft RW, Sander C, Vriend G.** The use of position-specific rotamers in model building by homology. *Proteins* 23: 415–421, 1995.
5. **Cokol M, Nair R, Rost B.** Finding nuclear localization signals. *EMBO Rep* 1: 411–415, 2000.
6. **Collin RW, Chellappa R, Pauw RJ, Vriend G, Oostrik J, van Drunen W, Huygen PL, Admiraal R, Hoefsloot LH, Cremers FP, Xiang M, Cremers CW, Kremer H.** Missense mutations in POU4F3 cause autosomal dominant hearing impairment DFNA15 and affect subcellular localization and DNA binding. *Hum Mutat* 29: 545–554, 2008.
7. **Cremers CW, Snik AF, Huygen PL, Joosten FB, Cremers FP.** X-linked mixed deafness syndrome with congenital fixation of the stapedial footplate and perilymphatic gusher (DFN3). *Adv Otorhinolaryngol* 61: 161–167, 2002.
8. **Cremers FP, Cremers FR, Kremer H.** POU3F4 and mixed deafness with temporal defect (DFN3). In: *Inborn Errors of Development*, edited by Epstein CJ, Erickson RP, and Wynshaw-Boris A. New York: Oxford University Press, 2008, p. 1042–1047.
9. **De Filippis V, Sander C, Vriend G.** Predicting local structural changes that result from point mutations. *Protein Eng* 7: 1203–1208, 1994.
10. **De Kok YJ, Merkx GF, van der Maarel SM, Huber I, Malcolm S, Ropers HH, Cremers FP.** A duplication/paracentric inversion associated with familial X-linked deafness (DFN3) suggests the presence of a regulatory element more than 400 kb upstream of the POU3F4 gene. *Hum Mol Genet* 4: 2145–2150, 1995.
11. **De Kok YJ, van der Maarel SM, Bitner-Glindzicz M, Huber I, Monaco AP, Malcolm S, Pembrey ME, Ropers HH, Cremers FP.** Association between X-linked mixed deafness and mutations in the POU domain gene POU3F4. *Science* 267: 685–688, 1995.
12. **Dominov JA, Miller JB.** POU homeodomain genes and myogenesis. *Dev Genet* 19: 108–118, 1996.
13. **Hara Y, Rovescalli AC, Kim Y, Nirenberg M.** Structure and evolution of four POU domain genes expressed in mouse brain. *Proc Natl Acad Sci USA* 89: 3280–3284, 1992.
14. **Hengen PN.** Methods and reagents. Purification of GST fusion proteins. *Trends Biochem Sci* 21: 400–401, 1996.
15. **Hertzano R, Dror AA, Montcouquiol M, Ahmed ZM, Ellsworth B, Camper S, Friedman TB, Kelley MW, Avraham KB.** Lhx3, a LIM domain transcription factor, is regulated by Pou4f3 in the auditory but not in the vestibular system. *Eur J Neurosci* 25: 999–1005, 2007.
16. **Hertzano R, Montcouquiol M, Rashi-Elkeles S, Elkon R, Yucel R, Frankel WN, Rechavi G, Moroy T, Friedman TB, Kelley MW, Avraham KB.** Transcription profiling of inner ears from Pou4f3(ddl/ddl) identifies Gfi1 as a target of the Pou4f3 deafness gene. *Hum Mol Genet* 13: 2143–2153, 2004.
17. **Hussain MA, Lee J, Miller CP, Habener JF.** POU domain transcription factor brain 4 confers pancreatic alpha-cell-specific expression of the proglucagon gene through interaction with a novel proximal promoter G1 element. *Mol Cell Biol* 17: 7186–7194, 1997.
18. **Kim J, Kim EY, Lee JS, Lee WS, Kim HN.** Temporal bone CT findings in Cornelia de Lange syndrome. *AJNR Am J Neuroradiol* 29: 569–573, 2008.
19. **Klemm JD, Rould MA, Aurora R, Herr W, Pabo CO.** Crystal structure of the Oct-1 POU domain bound to an octamer site: DNA recognition with tethered DNA-binding modules. *Cell* 77: 21–32, 1994.
20. **Le Moine C, Young WS 3rd.** RHS2, a POU domain-containing gene, and its expression in developing and adult rat. *Proc Natl Acad Sci USA* 89: 3285–3289, 1992.
21. **Malik KF, Kim J, Hartman AL, Kim P, Young WS 3rd.** Binding preferences of the POU domain protein Brain-4: implications for autoregulation. *Brain Res Mol Brain Res* 38: 209–221, 1996.
22. **Mathis JM, Simmons DM, He X, Swanson LW, Rosenfeld MG.** Brain 4: a novel mammalian POU domain transcription factor exhibiting restricted brain-specific expression. *EMBO J* 11: 2551–2561, 1992.
23. **Minowa O, Ikeda K, Sugitani Y, Oshima T, Nakai S, Katori Y, Suzuki M, Furukawa M, Kawase T, Zheng Y, Ogura M, Asada Y, Watanabe K, Yamanaka H, Gotoh S, Nishi-Takeshima M, Sugimoto T, Kikuchi T, Takasaka T, Noda T.** Altered cochlear fibrocytes in a mouse model of DFN3 nonsyndromic deafness. *Science* 285: 1408–1411, 1999.
24. **Morton NE.** Genetic epidemiology of hearing impairment. *Ann NY Acad Sci* 630: 16–31, 1991.
25. **Okazawa H, Imafuku I, Minowa MT, Kanazawa I, Hamada H, Mouradian MM.** Regulation of striatal D1A dopamine receptor gene transcription by Brn-4. *Proc Natl Acad Sci USA* 93: 11933–11938, 1996.
26. **Petersen MB, Wang Q, Willems PJ.** Sex-linked deafness. *Clin Genet* 73: 14–23, 2008.
27. **Phelps PD, Reardon W, Pembrey M, Bellman S, Luxom L.** X-linked deafness, stapes gushers and a distinctive defect of the inner ear. *Neuroradiology* 33: 326–330, 1991.
28. **Phippard D, Heydemann A, Lechner M, Lu L, Lee D, Kyin T, Crenshaw EB 3rd.** Changes in the subcellular localization of the Brn4 gene product precede mesenchymal remodeling of the otic capsule. *Hear Res* 120: 77–85, 1998.
29. **Phippard D, Lu L, Lee D, Saunders JC, Crenshaw EB 3rd.** Targeted mutagenesis of the POU-domain gene Brn4/Pou3f4 causes developmental defects in the inner ear. *J Neurosci* 19: 5980–5989, 1999.
30. **Reznikoff CA, Brankow DW, Heidelberger C.** Establishment and characterization of a cloned line of C3H mouse embryo cells sensitive to postconfluence inhibition of division. *Cancer Res* 33: 3231–3238, 1973.
31. **Riccomagno MM, Martinu L, Mulheisen M, Wu DK, Epstein DJ.** Specification of the mammalian cochlea is dependent on Sonic hedgehog. *Genes Dev* 16: 2365–2378, 2002.
32. **Vahava O, Morell R, Lynch ED, Weiss S, Kagan ME, Ahituv N, Morrow JE, Lee MK, Skvorak AB, Morton CC, Blumenfeld A, Frydman M, Friedman TB, King MC, Avraham KB.** Mutation in transcription factor POU4F3 associated with inherited progressive hearing loss in humans. *Science* 279: 1950–1954, 1998.
33. **Van Camp G, Smith RJH.** Hereditary Hearing Loss Homepage, http://webh01.ua.ac.be/hhh.
34. **Vriend G.** WHAT IF: a molecular modeling and drug design program. *J Mol Graph* 8: 52–56, 29, 1990.
35. **Weiss S, Gottfried I, Mayrose I, Khare SL, Xiang M, Dawson SJ, Avraham KB.** The DFNA15 deafness mutation affects POU4F3 protein stability, localization, and transcriptional activity. *Mol Cell Biol* 23: 7957–7964, 2003.
36. **Welter JF, Gali H, Crish JF, Eckert RL.** Regulation of human involucrin promoter activity by POU domain proteins. *J Biol Chem* 271: 14727–14733, 1996.